Journal of the Korean Physical Society, Vol. 51, No. 2, August 2007, pp. 475∼479

Optimal Molar Fractions of Ternary Zinc-Blende Terahertz Emitters

Minwoo Yi, Kanghee Lee and Jaewook Ahn*
Department of Physics, Korea Advanced Institute of Science and Technology, Daejeon 305-701

(Received 15 March 2007)

We report our calculation of optimal molar fractions in various ternary zinc-blende terahertz emitters that can produce terahertz radiation with enhanced powers when the wavelength of the pump laser is changed. While the momentum mismatch between the optical and the terahertz pulses in these non-resonant nonlinear materials was mainly used to understand the spectral and the transient shapes of the generated terahertz waves, the optimal molar fractions in compound semiconductor terahertz emitters were better determined with the full numerical calculations. To demonstrate the output power change and the sensitivity of the calculation, we performed numerical simulations of the optical rectification process during the optical and the terahertz wave propagations. The result suggests that the optimal Cd compositions in $Zn_{1-x}Cd_xTe$ are $x = 0.10$ at $\lambda = 820$ nm and $x = 0.65$ at $\lambda = 850$ nm and that the Te compositions in $ZnSe_{1-x}Te_x$ are $x = 0.6$ at $\lambda = 750$ nm and $x = 0.95$ at $\lambda = 820$ nm. This method could act as a powerful tool to optimally design various zinc-blende semiconductor compounds to generate terahertz waveforms.

PACS numbers: 07.57.Hm, 78.20.Jq, 42.65.Ky, 42.70.Nq
Keywords: Terahertz, Optical rectification, Phase-matching condition, Zinc-blende, $Zn_{1-x}Cd_xTe$, $ZnSe_{1-x}Te_x$

I. INTRODUCTION

Terahertz science and technology has attracted much interest because of their many up-and-coming applications in communications, material characterizations, biological and medical imaging, and high-precision spectroscopy of molecules [1–8]. Especially, terahertz time-domain spectroscopy (THz-TDS) has become widely used for the measurement of absorption and dispersion of materials in the terahertz frequency range. The two-dimensional measurement of THz-TDS has made the imaging of biological tissues and chemical compositions in such a frequency range possible. Auston switching is the most widely used method of terahertz generation. In that method, laser pulses illuminate a strip-line electrically-biased antenna drawn on a semiconductor substrate to accelerate the current surge and simultaneously to generate terahertz electric radiation.

More lately, optical rectification has become one of the popular methods of teraertz generation. During the optical rectification process, two optical waves with angular frequency ω_{opt} interact with each other in a nonlinear medium, generating a dc polarization $P(\Omega)$ through the second-order nonlinear susceptibility $\chi^{(2)}(\Omega = 0;\ \omega_{opt}, -\omega_{opt})$. In general, optical rectification produces an electric polarization with a low frequency in a nonlinear medium. If the ultrashort optical pulse contains various spectral components and there are beatings between the different frequency components in a single ultrashort pulse, the beatings will generate far- to mid-IR radiation. The components at angular frequencies $\Omega \neq 0$ act as sources of terahertz radiation. This process, $\chi^{(2)}(\Omega;\ \omega_{opt}, -\omega_{opt} - \Omega)$, may be interpreted as difference frequency mixing between the spectral components of the ultrashort optical input pulse. The upper bound of Ω is limited by the bandwidth $\triangle\omega_{opt}$ of the ultrashort optical pulse. The generated electric temporal waveform is the envelope of the ultrashort optical pulse in a nonlinear electro-optical medium.

The nonlinear polarization induced by a single ultrashort pulse with a complicated electric field may be written as [9]

$$P(\Omega) = \varepsilon_0 \chi^{(2)} \int_{-\infty}^{+\infty} E(\omega_{opt}) E^*(\omega_{opt} - \Omega) d\omega_{opt}. \quad (1)$$

In the above equation, the dispersion of the nonlinear coefficient is not considered. The frequency components of this equation may be expressed as

$$P(t) = \varepsilon_0 \chi^{(2)} E(t) E^*(t) \propto \chi^{(2)} I(t). \quad (2)$$

This time domain equation shows that the pulse width of the generated radiation depends on that of the optical pump pulse. By changing the shape of the pumping laser pulse [10] or by designing the material properties by mix-

*E-mail: jwahn@kaist.ac.kr

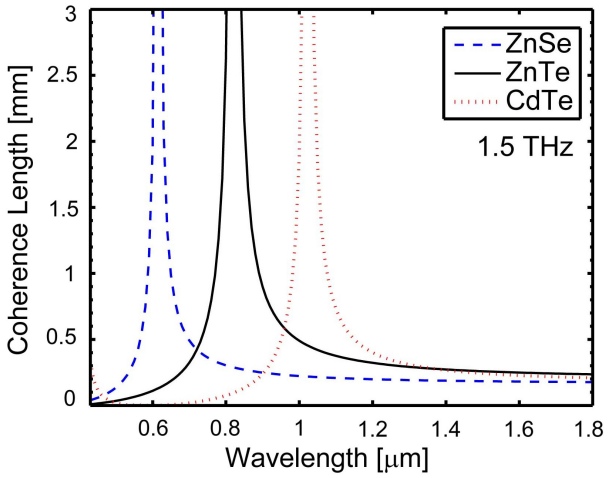

Fig. 1. Coherence length $l_c(\lambda_{opt};\Omega)$ measured at the generated terahertz frequency $\Omega = 1.5$ THz as a function of the optical wavelength λ_{opt}. From left to right: ZnSe, ZnTe and CdTe.

ing or alternating materials [11], one may be able to produce this electric popularization on demand to achieve versatile terahertz shapes. For more recent developments and applications in terahertz science and technology, the ability to generate a variety of temporal and spectral terahertz shapes is desired. Some of those tailored terahertz pulses have been utilized for coherent control of carrier dynamics in semiconductor nanostructures [12] and for quantum systems such as Rydberg atoms [13].

II. OPTIMAL COMPOUNDS FOR TERAHERTZ GENERATIONS

Several electro-optic materials, including ZnTe, CdTe, GaP, $LiNbO_3$, and even organic crystals, have been considered as terahertz emitters and sensors [11, 14–19]. Among these materials, due to the high efficiency of the nonlinear process, <110>-oriented zinc-blende semiconductors, including ZnTe, CdTe, and GaP, are widely accepted for the generation and detection of terahertz pulses. Especially, ZnTe has been accepted as one of the most appropriate electro-optic materials for terahertz generation and sensing to be coupled with Ti:Sapphire laser systems [20].

Figure 1 shows the coherence lengths calculated at the generated terahertz frequency of 1.5 THz as a function of the optical wavelength for several II-VI semiconductors: ZnSe, ZnTe, and CdTe. Around the optical wavelength of 800 nm, the wavelength of a Ti:Sapphire laser tuned to produce the maximum power, ZnTe has the largest coherence length. This is the reason IR femtosecond pulses from the Ti:Sapphire laser are used with ZnTe crystals with <110>-orientations for generating terehertz radiations. Outside the wavelength range of ∼800 nm, the phase velocity $v_{ph}(\Omega)$ in the terahertz range is smaller than $v_g(\lambda_{opt})$, resulting in a shorter coherence length. On the other hand, for CdTe, the peak of the coherence curve is located at ∼1100 nm, and for ZnSe, it is at ∼600 nm, raising the possibility of using $Zn_{1-x}Cd_xTe$ and $ZnSe_{1-x}Te_x$ compounds as efficient terahertz emitters coupled with ligh sources of 600 – 1000 nm.

Our motivation in this work is to use compound materials for terahertz generation, specially for engineering the spectral and the temporal shapes of the terahertz pulses. Ternary compounds with large electro-optic coefficients are expected to produce various shapes at various excitation wavelengths. In this study, we calculate the optimal molar fractions x in the compound materials: $Zn_{1-x}Cd_xTe$ and $ZnSe_{1-x}Te_x$. The spectral components of the terahertz pulses generated from these compound emitters are computed by numerically solving the nonlinear Maxwell equation in the spatio-temporal domain [10, 21]. The calculation model mainly deals with the momentum mismatch between the optical pump pulse and the terahertz pulse during the generation process [20]. The calculated influence of the Cd molar fraction gives an understanding of a former study of $Zn_{1-x}Cd_xTe$ with the optical excitation close to 820 nm [22]. In this former study, Liu *et al.*, however, considered only the phase-matching condition to account for their experiment results. The influence of other conditions, such as the crystal thickness and the duration of optical laser pulses, must also be taken into account for the actual shapes of generated terahertz pulses [23].

III. MODEL CALCULATION

The efficiency of the terahertz pulse generation strongly depends on the momentum mismatch between the optical and the terahertz pulses in the nonlinear medium. The momentum mismatch condition for the wavelength at different frequencies is

$$\triangle k = k(w_{opt} + \Omega) - k(w_{opt}) - k(\Omega) = 0. \quad (3)$$

The momentum mismatch Δk influences the inverse of the coherence length l_c for the optical rectification process in a material with dispersion at optical frequencies. The coherence length l_c, which depends on the efficiency of terahertz generation, is given by

$$l_c(\Omega;\lambda_{opt}) = \frac{\pi}{\triangle k} = \frac{\pi c}{\Omega\,|N_{eff}(\lambda_{opt}) - n_{THz}(\Omega)|}, \quad (4)$$

where $N_{eff}(\lambda_{opt})$ is the effective refractive index for an optical pump beam with a wavelength of λ_{opt} [20],

$$N_{eff}(\lambda_{opt}) = n_{opt}(\lambda_{opt}) - \lambda_{opt}\frac{dn_{opt}(\lambda)}{d\lambda}\,|_{\lambda_{opt}}\,. \quad (5)$$

The amplitude of each spectral component of the local terahertz field $E^{THz}(\Omega, z)$ is computed by solving

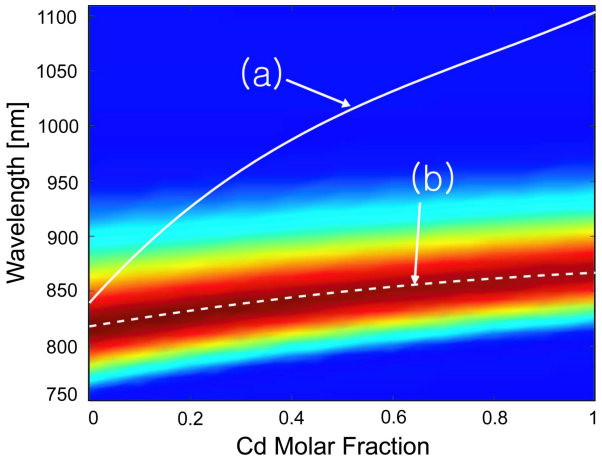

Fig. 2. Total terehertz power from a 2-mm-thick $Zn_{1-x}Cd_xTe$ emitter, calculated with respect to the change in the pump laser is wavelength and the Cd molar fraction. The solid line (a) obtained from the condition that the momentum mismatch $\triangle k$ becomes zero is different from the dashed line (b), the maxima of the terahertz power measured from the full calculation.

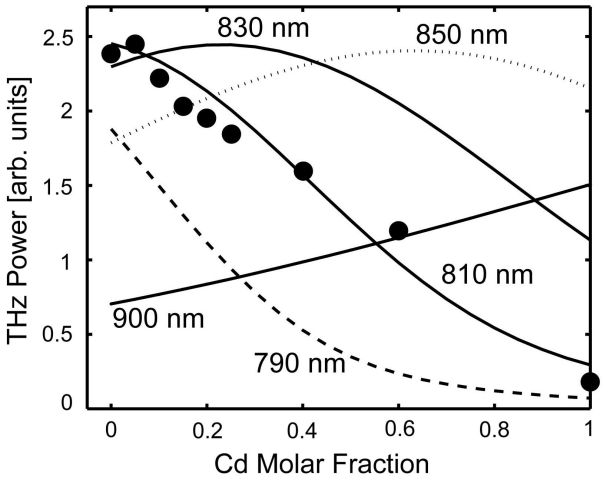

Fig. 3. Calculated terahertz power as a function Cd molar fraction for $Zn_{1-x}Cd_xTe$ emitters. The wavelength of the ultrashort pump pulse is changed from 810 nm to 900 nm. The results of Liu *et al.* shown with filled circles [22] are comparable with the calculated power at a pump laser wavelength of 810 nm.

the nonlinear Maxwell equation in the spatio-temporal Fourier domain [21]:

$$\frac{\partial^2}{\partial z^2}E^{THz}(\Omega,z)+\varepsilon(\Omega)\frac{\Omega^2}{c^2}E^{THz}(\Omega,z) = -\frac{4\pi\Omega^2}{c^2}P(\Omega,z), \quad (6)$$

where the polarization $P(\Omega,z)$ is the product of the second-order nonlinear susceptibility $\chi^{(2)}(\Omega)$ and the Fourier components of the intensity of the pump laser pulse:

$$P(\Omega,z)=\chi^{(2)}(\Omega)I(\Omega)\exp[i\Omega z/v_g]. \quad (7)$$

Here, v_g is the group velocity of the optical pulse, and if the pump laser pulse is assumed to be a Gaussian pulse with a pulse width τ_{opt}, the Fourier component of the intensity of the pump laser pulse may be expressed as $I(\Omega)=I_o\exp[-(\tau_{opt}\Omega)^2/2]$.

The solution for this nonlinear Maxwell equation is obtained at each point in the crystals as [10]

$$E^{THz}(\Omega,z)\propto\Omega^2\chi^{(2)}(\Omega)I(\Omega)z\,\mathrm{sinc}\left[\frac{\Delta kz}{2}\right]. \quad (8)$$

We obtain the amplitude of each spectral terahertz component by integrating Eq. (8) over the crystal thickness. In order to obtain terahertz spectral shapes appropriate for some particular purpose and to maximize $E^{THz}(\Omega,z)$ for a terahertz frequency range, one must choose the wavelength λ_{opt} and the duration τ_{opt} of the ultrashort optical pulse and the properties of the crystal, such as the kind of material, the molar fraction ratio, and the crystal thickness. In this study, we considered the optimal molar fraction x in compound materials such as $Zn_{1-x}Cd_xTe$ and $ZnSe_{1-x}Te_x$ for terahertz emitters.

IV. COHERENCE LENGTH AND TOTAL TERAHERTZ POWER

1. $Zn_{1-x}Cd_xTe$ THz Emitters

For the calculations, the NIR indexes of refraction, n_{opt}, of $Zn_{1-x}Cd_xTe$ measured at room temperature are obtained from the model dielectric function (MDF) [24]. The refractive indexes in the FIR region, n_{THz}, are obtained from a linear interpolation of the data taken from the refractive indexes of ZnTe and CdTe in Ref. 25. Figure 2 shows the calculated total terahertz power emitted from a 2-mm-thick $Zn_{1-x}Cd_xTe$ with respect to changes in the Cd composition. The excitation pulse from a Ti:Sapphire laser system has Gaussian pulse envelope with 155 fs pulse duration. The solid line (a) in Figure 2 is obtained from the condition that the momentum mismatch $\triangle k$ becomes zero or

$$\triangle k=N_{eff}(\lambda_{opt})-n_{THz}(\Omega)=0. \quad (9)$$

The dashed line (b) in the same figure is the maxima of the terahertz power drawn in the 2-dimensional mesh of the Cd molar fraction and the excitation pulse wavelength. In fact, the wavelength-dependent phase-matching condition considered in (a) should not be the same as the result in (b), which calculates the total terhaertz power. Especially, when a crystal with the given thickness is used, the terahertz radiation with a very narrow frequency window that satisfies (a) may produce a lot smaller power than the terahertz radiation generated when entering and exiting crystal surfaces with a thickness of an effective coherence length. The total terahertz power dramatically changes as a function of pump

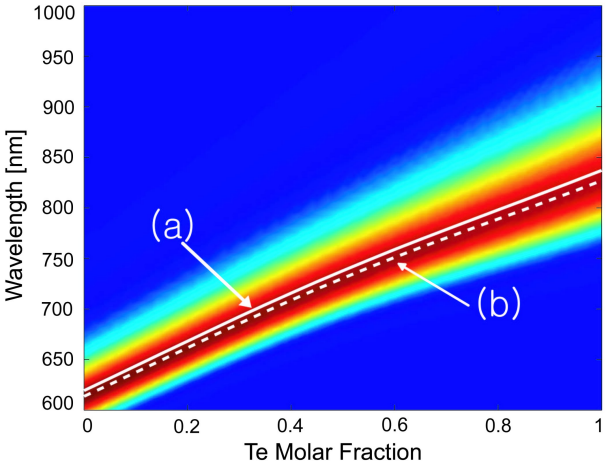

Fig. 4. Calculated total terahertz power from a 2-mm-thick $ZnSe_{1-x}Te_x$ emitter, calculated with respect to the change in the pump laser's wavelength and the Te molar fraction. The solid line (a) is obtained when the momentum mismatch $\triangle k$ becomes zero and the dashed line (b) is the total terahertz power maxima at a specific Te molar fraction.

laser wavelength and Cd composition in the $Zn_{1-x}Cd_xTe$ emitter. The difference between the solid line and the dashed line in Figure 2 shows that the generated terahertz field strongly depends on the crystal properties, such as the thickness and the molecular composition. In previous studies, Liu *et al.* found that the optimal Cd composition was $x = 0.05$ for a 820-nm pump pulse [22]. As shown in Figure 3, the results from Liu *et al.* are comparable with the calculation, and we determine the optimal molar fraction from the model, as shown in Figure 3. The result suggests that the optimal Cd compositions in $Zn_{1-x}Cd_xTe$ are $x = 0.10$ at $\lambda = 820$ nm and $x = 0.65$ at $\lambda = 850$ nm.

2. $ZnSe_{1-x}Te_x$ THz Emitters

Similarly, we have studied the nature of terahertz wave generation in $ZnSe_{1-x}Te_x$ THz emitters. The room temperature indexes of refraction of $ZnSe_{1-x}Te_x$ in the NIR and the FIR regions are obtained from Ref. 26. The refractive indexes of ZnTe and ZnSe in Ref. 25 and 27 are used to obtain the refractive indexes n_{THz} of $ZnSe_{1-x}Te_x$. Figure 4 shows the change in the calculated terahertz power from a 2-mm-thick $ZnSe_{1-x}Te_x$ emitter for various Te compositions. In this series of $ZnSe_{1-x}Te_x$ compounds, the solid line (a), which considers phase-matching, and the dashed line in (b) from the full calculation overlap with each other. If we consider the optimal Te compositions for maximal terahertz power in $ZnSe_{1-x}Te_x$ compounds, we get $x = 0.6$ at $\lambda = 750$ nm and $x = 0.95$ at $\lambda = 820$ nm.

V. CONCLUSION

In this study, we have considered ternary zinc-blende terahertz emitters and their optimal molar compositions for maximum output power. The numerical calculations using the nonlinear Maxwell equations show that the output terahertz spectrum sensitively depends on the pump laser wavelength and the composition of the emitter compound. Contrary to the previous study on similar materials by Liu et al., our calculations show that the optimal molar fractions in $Zn_{1-x}Cd_xTe$ compounds are $x = 0.10$ at $\lambda = 820$ nm and $x = 0.65$ at $\lambda = 850$ nm. This result allows one to use the full IR spectral range of Ti:Sapphire lasers for pumping various $Zn_{1-x}Cd_xTe$ terahertz emitters. Similarly, the Te compositions in $ZnSe_{1-x}Te_x$ are $x = 0.6$ at $\lambda = 750$ nm and $x = 0.95$ at $\lambda = 820$ nm. Therefore, further experimental studies on optimal compounds for terahertz wave generation are expected. We have shown that in certain materials, a numerical analysis beyond simple phase-matching is necessary to design an optimal terahertz wave emitter. Similarly, other binary and ternary zinc-blende crystals, such as ZnS, GaP, $Zn_{1-x}Cd_xSe$, $Zn_xMg_{1-x}Te$ and $Zn_xMn_{1-x}Te$ and organic crystal DAST may be analyzed using this method.

ACKNOWLEDGMENTS

This work was supported by the Korea Research Foundation Grant funded by the Korean Government (MOHERD) (KRF-2005-205-C00024) and by the Korean Ministry of Commerce, Energy, Industry and Energy (MOCIE) (B0008183-2006-04).

REFERENCES

[1] D. S. Citrin and S. Hughes, Appl. Phys. Lett. **78**, 1805 (2001).
[2] C. Kang, I. H. Maeng, S. J. Oh, J.-H. Son, T.-I. Jeon, K. H. An, S. C. Lim and Y. H. Lee, Appl. Phys. Lett. **87**, 041908 (2005).
[3] V. K. Thormsølle, R. D. Averitt, T. Shibauchi, M. F. Hundley and A. J. Taylor, Phys. Rev. Lett. **97**, 237001 (2006).
[4] J. L. Johnson, T. D. Dorney and D. M. Mittleman, Appl. Phys. Lett. **78**, 835 (2001).
[5] C. Ronne, P. Strand and S. R. Keiding, Phys. Rev. Lett. **82**, 2888 (1999).
[6] R. Parthasarathy, T. Globus, T. Khromova, N. Swami and D. Woolard, Appl. Phys. Lett. **87**, 113901 (2005).
[7] H. J. Cha, Y. U. Jeong, S. H. Park, B. C. Lee and S.-H. Park, J. Korean Phys. Soc. **49**, 354 (2006).
[8] Y.-S. Jin, G.-J. Kim, S.-G. Jeon, C.-H. Shon and S.-S. Jung, J. Korean Phys. Soc. **48**, 603 (2006).
[9] A. Bonvalet, M. Joffre, J. L. Martin and A. Migus, Appl. Phys. Lett. **67**, 2907 (1995).

[10] J. Ahn, A. Efimov, R. Averitt and A. Taylor, Opt. Express **11**, 2486 (2003).
[11] N. Amer, W. C. Hurlbut, B. J. Norton and Y.-S. Lee, Appl. Opt. **45**, 1857 (2006).
[12] B. E. Cole, J. B. Willams, B. T. King, M. S. Sherwin and C. R. Stanley, Nature **410**, 60 (2001).
[13] J. Ahn, D. N. Hutchinson, C. Rangan and P. H. Buchsbaum, Phys. Rev. Lett. **86**, 1179 (2001).
[14] C. Winnewisser, P. Uhd Jepson, M. Schall, V. Schyja and H. Helm, Appl. Phys. Lett. **70**, 3069 (1997).
[15] Q. Wu and X.-C. Zhang, Appl. Phys. Lett. **68**, 1604 (1996).
[16] Q. Wu and X.-C. Zhang, Appl. Phys. Lett. **71**, 1285 (1997).
[17] A. Rice, Y. Jin, X. F. Ma, X.-C. Zhang, D. Bliss, J. Larkin and M. Alexander, Appl. Phys. Lett. **64**, 1324 (1994).
[18] M. Schall, M. Walther and P. Uhd Jepsen, Phys. Rev. B **64**, 094301 (2001).
[19] X. Xie, J. Xu and X.-C. Zhang, Opt. Lett. **31**, 978, (2006).
[20] A. Nahata, A. S. Weling and T. F. Heinz, Appl. Phys. Lett. **69**, 2321 (1996).
[21] J.-P. Caumes, L. Videau, C. Rouyer and E. Freysz, Phys. Rev. Lett. **89**, 047401 (2002).
[22] K. Liu, H. S. Kang, T. K. Kim and X.-C. Zhang, Appl. Phys. Lett. **81**, 4115 (2002).
[23] M. Yi, K. Jang, I. Maeng, J.-H. Son and J. Ahn, *Quantum Electronics and Laser Science Conference* (Blatimore, 2007).
[24] E. M. Larramendi, E. Puron and O. de Melo, Semicond. Sci. Technol. **17**, 8 (2002).
[25] M. Schall, H. Helm and S. R. Keiding, Int. J. Infrared and Millimeter Waves **20**, 595 (1999).
[26] X. Liu and J. K. Furdyna, J. Appl. Phys. **92**, 7754 (2004).
[27] E. D. Palik, *Handbook of Optical Constants of Solid*, Vol. 2. (Academic Press, Boston, 1991).